

## Size Resolved Kinetics of Nickel Nanoparticle Oxidation by Ion-Mobility Classification

*L. Zhou, A. Rai, N. Piekielek, X.F. Ma and M. R. Zachariah*

*Department of Mechanical Engineering and Department of Chemistry and Biochemistry  
University of Maryland, College Park, 20742, USA*

### 1. Introduction

Recent advancement on field of so called “nanoenergetic” materials are focused on either enhancing or tuning reactivity<sup>1</sup>. On one level this issues reduces to a length-scale argument, whereby smaller fuel/oxidizer combinations result in smaller diffusion lengths and therefore higher reactivity. On another level, this discussion leads to choices of other materials beyond aluminum as the primary thermite based fuel to Ti, or Ni, or even metal based composites such as Ni/Al. While the oxidation of Ni metal in form of bulk sample or thin films has been studied for over a century, there are only a few studies on the oxidation of nickel nanoparticles and most of the studies were carried out by using conventional dynamic thermal techniques such as thermogravimetry. It is well know that those methods are greatly influenced by heat and mass transfer effects such that the results are biased by experimental artifacts<sup>2, 3</sup>. In this work we employ aerosol based techniques to study the oxidation kinetics of Ni nanoparticles. The basic idea of the experiment approach is to prepare Ni particles of characterized size (i.e. Monodisperse), and monitor changes during oxidation in free-flight (i.e. no substrate). The study consists of two experiments, a Tandem Differential Mobility Analyzer (DMA) system<sup>4-7</sup> is used to measure the size change after oxidation, while the mass change is tracked by a DMA-APM (Aerosol Particle Mass Analyzer) system<sup>8-10</sup>. This technique allow a direct measure of mass and volume change of individual particles and thus enables us to explore the intrinsic reactivity of nanoparticles with minimizing the sampling error introduced by mass and heat transfer. The mass and size changes of nanoparticles are studied from room temperature to 1100C. The average density obtained show the nickel nanoparticle oxidation process can be correlated to the formation of both NiO and Ni<sub>2</sub>O<sub>3</sub> and a phase change region where both the oxidation of nickel and thermal decomposition of Ni<sub>2</sub>O<sub>3</sub> to NiO occur simultaneously. The reaction kinetics parameters (activation energy and effective diffusion coefficient) were then extracted from the experiment data as a function of particle size.

### 2. Experimental Approach

In this work, high purity nickel nanoparticles were prepared in an oxygen free environment using gas-phase thermal pyrolysis of nickel carbonyl as shown in Figure 1.

The primary analytical tools employed in the experiments were a tandem differential mobility analyzer system (TDMA)<sup>4-7</sup> and DMA-APM (aerosol particle mass analyzer) systems<sup>8-10</sup>. In the experiments, DMA-1 is used as a band pass-filter to create the monodisperse particle source, by selecting particles with same electrical mobility size. A second DMA was operated in voltage-step mode with a condensation particle counter (CPC) as a particle size distribution measurement tool to track the size change after the oxidation process. In a parallel experiment the change in particle mass after oxidation was measured by an aerosol particle mass analyzer (APM) coupled with a CPC.

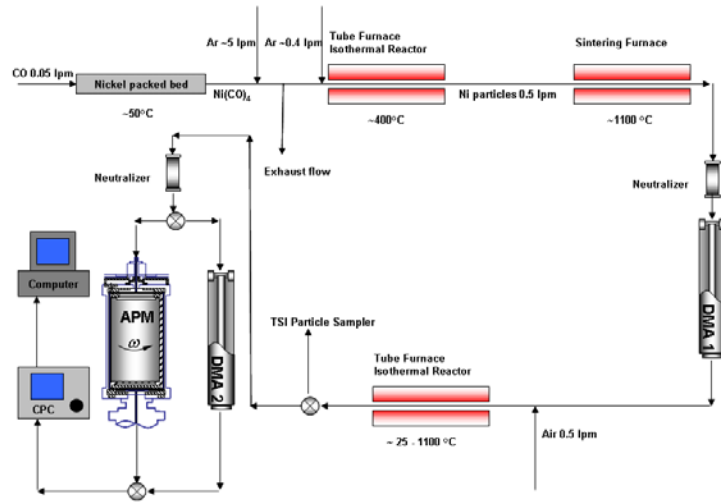


**Figure 1: Schematic of Ni generation and oxidation experiment.**

### 3. Size and Mass Measurements of Nickel Nanoparticle Oxidation

In this study, mobility sizes of 40, 62, 81, and 96 nm spherical nickel particles were obtained for oxidation study. Size selected particles mixed with air and oxidized, following which the size or mass of the reacted particles is measured by a second DMA or APM. The TDMA experimental results of size change  $\Delta D_p$  in Figure 2 (a) show that the particles size first increases as we increase the furnace temperature, and further increases in the reaction temperature, result in decreases in particle size.

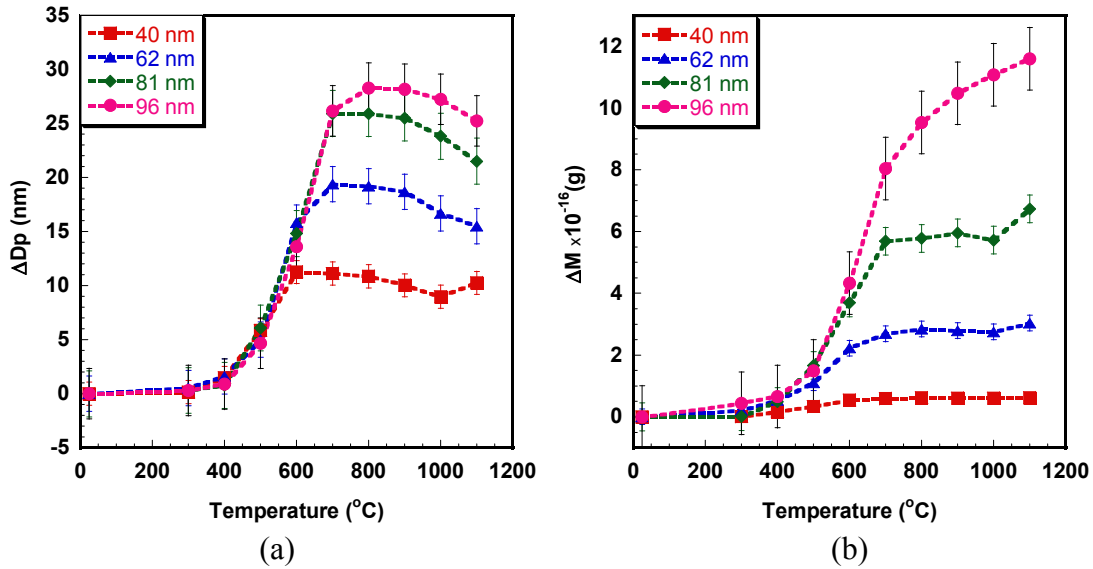


Figure 2 the change of (a) particle size and (b) particle mass as function of oxidation temperatures.

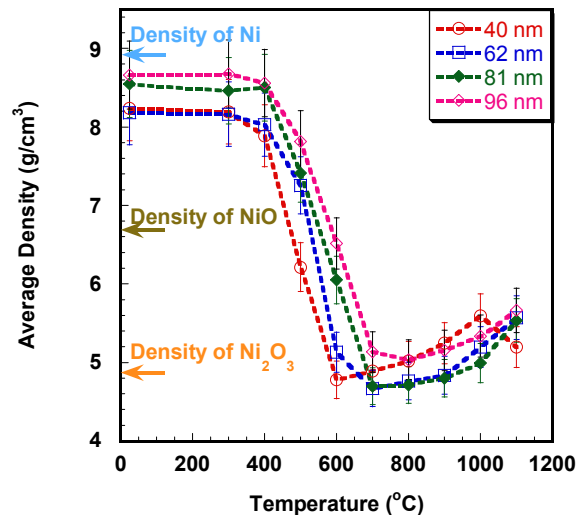


Figure 3 Average Density measured using DMA-APM setup

The APM measured mass change  $\Delta M$  are shown in figure 2 (b). The average density profiles of reacted particles are calculated and shown in figure 3, We find that as the furnace temperature increases, the average density of the reacted particles decreased monotonically to 4.7-5.0  $\text{g}/\text{cm}^3$ , consistent with the density of  $\text{Ni}_2\text{O}_3$  (4.84  $\text{g}/\text{cm}^3$ ). At higher temperatures the particle density increases to 5.5-5.7  $\text{g}/\text{cm}^3$  and at the highest temperature investigated is roughly at a density half way between  $\text{NiO}$  (6.67  $\text{g}/\text{cm}^3$ ) and  $\text{Ni}_2\text{O}_3$  (4.84  $\text{g}/\text{cm}^3$ ). The oxidation to form  $\text{Ni}_2\text{O}_3$  should be dominant in the low temperature region while the process of formation of the two types of oxides, and the phase transition are coupled at higher temperatures.

#### 4. Size-resolved Oxidation Kinetics of Nickel Nanoparticles

The well known diffusion controlled shrinking core model is employed in this work to extract the reaction rate constant. At steady state the mass change rate for the reacted nickel nanoparticle is

$$\frac{dM}{dt} = 4\pi M_{O_2} De Co_2 \frac{r_1 r_2}{r_2 - r_1} \quad (1)$$

where  $r_1, r_2$  are the radius of the nickel core, and the reacted particle radius.  $De$  is the diffusion coefficient for ions diffusion in oxide layer.  $Co_2$  is the oxygen molar concentration in gas.  $M_{O_2}$  is the molecular weight of oxygen. To simplify the problem we approximate the instantaneous mass changing rate with the average mass changing rate by using the mass change measured from the APM. The size-resolved activation energies are obtained from an Arrhenius plot as shown in figure 4(a) and the effective diffusion coefficients of oxidation process were plotted in figure 4 (b). Two different regions can be distinguished from the Arrhenius plot 4 (a), as the oxidation process transitions to a phase change region. The calculated activation energies at low temperature region decrease from 54 KJ/mol to 35 KJ/mol as the particle mobility size decrease from 96 nm to 40 nm. The size effect on the activation energy observed here may be explained by the enhanced surface area-to-volume ratio with decreasing particle mobility size.

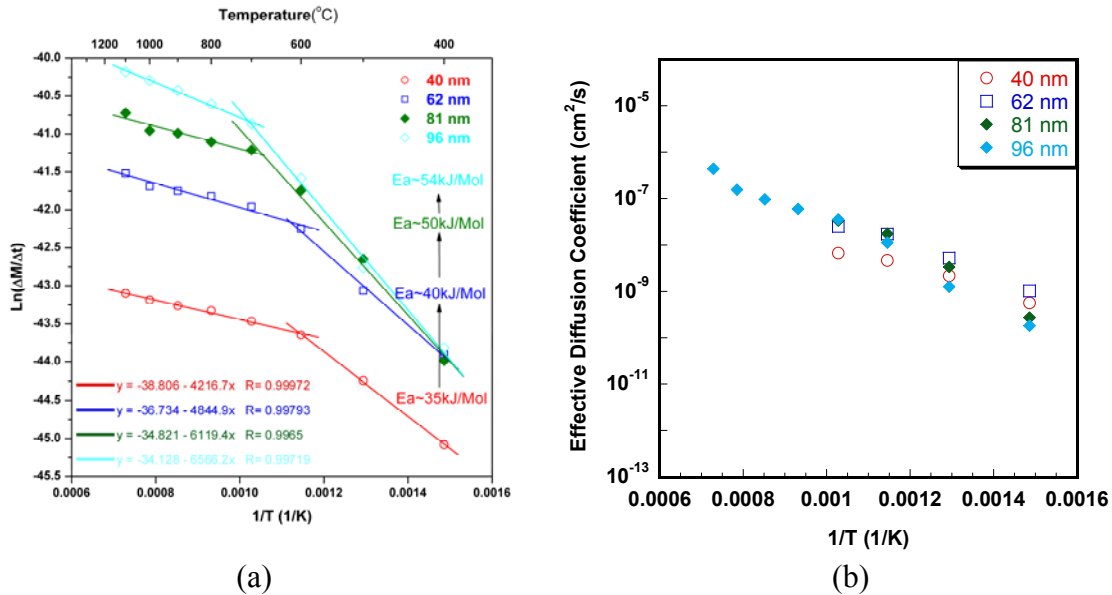


Figure 4 (a) Arrhenius plots of average mass changing rate as a function of inverse temperature (b) the effective diffusion coefficient of nickel nanoparticles oxidation

#### 5. Concluding Remarks

We applied an online aerosol based TDMA and DMA-APM methods to study oxidation and reactivity of nickel nanoparticles. The experimental data can be divided into an

oxidation region and a phase transit region. We found that the activation energy of oxidation process decreased from 54 KJ/mol to 35 KJ/mol as the particle mobility size decrease from 96 nm to 40 nm.

## References

- (1) A. Prakash, A. M., and M.R. Zachariah *Advanced Materials* **2005**, *17*, 900-903.
- (2) Park, K.; Lee, D.; Rai, A.; Mukherjee, D.; Zachariah, M. R. *J. Phys. Chem. B* **2005**, *109*, 7290-7299.
- (3) Mahadevan, R.; Lee, D.; Sakurai, H.; Zachariah, M. R. *J. Phys. Chem. A* **2002**, *106*, 11083-11092.
- (4) Knutson, E. O.; Whitby, K. T. *Journal of Aerosol Science* **1975**, *6*, 443-451.
- (5) Kim, S. H.; Fletcher, R. A.; Zachariah, M. R. *Environmental Science & Technology* **2005**, *39*, 4021-4026.
- (6) Jung, H.; Kittelson, D. B.; Zachariah, M. R. *Combustion and Flame* **2005**, *142*, 276-288.
- (7) Higgins, K. J.; Jung, H. J.; Kittelson, D. B.; Roberts, J. T.; Zachariah, M. R. *Journal of Physical Chemistry A* **2002**, *106*, 96-103.
- (8) Park, K.; Rai, A.; Zachariah, M. R. *Journal of Nanoparticle Research* **2006**, *8*, 455-464.
- (9) Park, K.; Kittelson, D. B.; Zachariah, M. R.; McMurry, P. H. *Journal of Nanoparticle Research* **2004**, *6*, 267-272.
- (10) Ehara, K.; Hagwood, C.; Coakley, K. J. *Journal of Aerosol Science* **1996**, *27*, 217-234.